Evaluation of Damage Tolerance in Aircraft Structures

H. I. McHenry*
National Bureau of Standards, Boulder, Colo.
and
E. K. Hensley†
General Dynamics/Fort Worth Division, Fort Worth, Texas

The specific requirements and the evaluation procedures used to qualify the damage tolerance of two competing wing carrythrough structure designs are reviewed. One design is principally beta-processed 6A1-4V titanium in a fail safe configuration, and the other is principally 10 Ni steel in a monolithic configuration. Fail safe analyses were conducted using finite element models with individual elements reduced in size or eliminated to simulate failure. Crack arrest was evaluated experimentally on panels with brazed stiffeners. Crack growth analyses were based on extensive test data and the Wheeler retardation model.

Introduction

CURRENT military specifications require an analytical and experimental assessment of the damage tolerance of the airframe. Critical primary structure must be qualified as fail-safe or safe-crack-growth structure. In this paper the specific requirements and the evaluation procedures used in the Advanced Metallic Air Vehicle Structure (AMAVS) Program are presented.

The purpose of the AMAVS Program, sponsored by the Air Force Flight Dynamics and Materials Laboratories (AFFDL and AFML), is to demonstrate that advanced technology can increase the structural efficiency, integrity, and reliability of future Air Force systems. A comparative approach was used to demonstrate that advanced materials, manufacturing, and structures technology can improve aircraft structures. The wing carrythrough structure (WCTS) of a variable wing-sweep airplane serves as the baseline for comparison. The WCTS designed in the AMAVS Program is required to meet all geometrical and functional interface requirements of the baseline structure. It must be designed to the same load requirements and criteria as the baseline.

The paper presents the damage tolerance requirements and the procedures used to qualify the damage tolerance of two competing WCTS designs—on fail-safe and the other monolithic. In both cases, a high level of damage tolerance is demonstrated.

Damage Tolerance Requirements

A rigorous set of damage tolerance design requirements was applicable to both the baseline and the AMAVS designs. These requirements augment standard Air Force strength and fatigue requirements by specifying residual strength, rigidity and life requirements for primary structure containing initial flaws.

Fail-safe requirements depend on whether or not the structure is readily accessible for inspection, i.e., can be inspected without removal of fasteners (except for access panels), paint, or sealant. Fail-safe structures which are readily inspectable must have residual strength in excess of limit load capacity and residual fatigue life in excess of ¼ service life after failure of a principal element. The structure remaining after failure of the first element is assumed to be without flaws. Dynamic release of energy during element failure is accounted for by use of a dynamic factor. A factor of 1.15 is applied to the maximum load in the fatigue spectrum when computing stresses adjacent to the failed member. The residual fatigue life of ¼ service life is computed using fatigue analysis procedures with a scatter factor of 1 for integral fuel tank structures which allow leakage to exterior surfaces prior to fracture and a scatter factor of 2 for all other structure.

Fail-safe structures which are not readily inspectable must have a combination of safe crack growth prior to element failure plus residual fatigue life after element failure that exceeds 1 service life. The safe crack growth interval is computed using an assumed initial flaw that is 0.15 in. in its critical dimension and located in the most unfavorable place with respect to the applied stress, the material properties, and the chemical and thermal environment. The residual fatigue life is computed using fatigue analysis procedures with a structure remaining after failure of the first element which is assumed to be without flaw.

Monolithic structure or multimember structure which does not meet the fail-safe requirements must be designed so that initial cracks will not grow to critical size during one service life. The safe crack growth interval is computed using an assumed initial flaw that is 0.15 in. in its critical dimension and located in the most unfavorable place with respect to the applied stress, the material properties, and the chemical and thermal environment.

Wing Carrythrough Structure Designs

Two WCTS configurations were completed through the detail design phase of the AMAVS Program. These configurations can be characterized as 1) a fail safe titanium design and 2) a monolithic steel design. They are shown in Figs. 1 and 2.

A distinguishing feature of the titanium design is the multi-element brazed lower plate and lugs. The titanium alloy selected for this design is Ti-6A1-4V (beta processed and mill annealed) because of its excellent fracture resistance and its compatibility with the brazing cycle. Crack arrest capability of the brazed joints permits each bay of the lower plate to be considered as an individual element for fail-safe analysis. Titanium is also used extensively in the upper cover and lugs,

Presented as Paper 74-347 at the AIAA/ASME/SAE 15th Structures, Structural Dynamics and Materials Conference, Las Vegas, Nev., April 17-19, 1974; submitted May 6, 1974; revision received September 9, 1974. This work was conducted as part of the Advanced Metallic Air Vehicle Structure Program sponsored by the Air Force Flight Dynamics and Materials Laboratories under Contract F33615-73-C-3001.

Index categories: Aircraft Structural Design (Including Loads); Aircraft Structural Materials; Materials, Properties of.

*Metallurgist.

†Design Specialist.

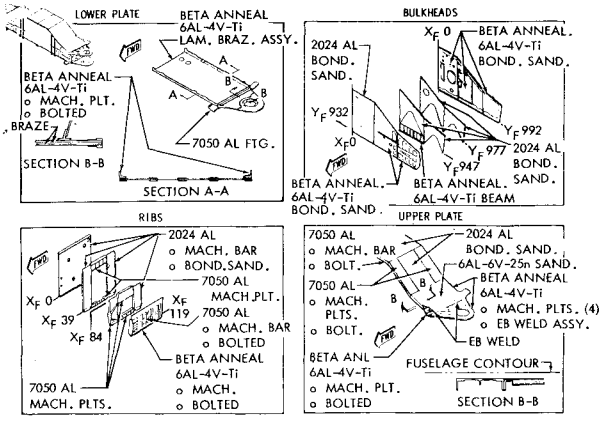

Fig. 1 Fail-safe titanium wing carrythrough structure.

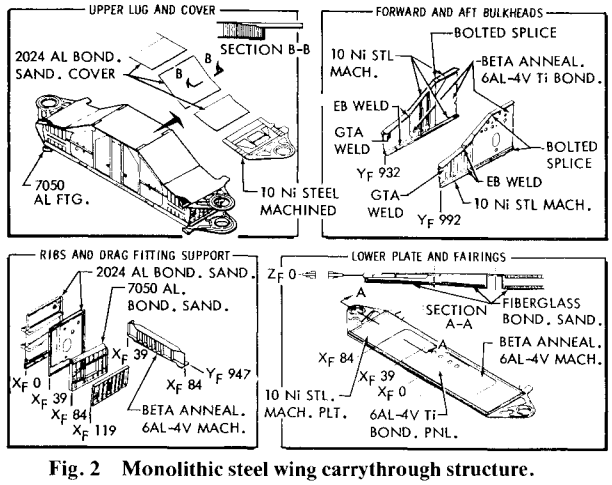

Fig. 2 Monolithic steel wing carrythrough structure.

the forward and aft bulkheads, the closure rib, and in several fittings. Aluminum alloy 7050 is used in the internal ribs, upper cover, and bulkheads.

The monolithic steel design utilizes a single steel plate for the lower lugs and lower plate. The alloy selected for this plate is 10 Ni steel (HY180) because it exhibits ductile fracture behavior in the relatively thick sections (1.5 in.) used throughout the lower plate. The fracture behavior is ductile over the range of temperatures (-65 to +140°F) and strain rates ($\epsilon \approx 10^{-2}$/sec) applicable to the WCTS. The 10 Ni steel is also used in the upper lugs and the more highly loaded portions of the upper cover and the forward and aft bulkheads. Beta annealed 6A1-4V titanium is used in the central portions of the lower plate bulkheads, the closure rib, and fittings. Aluminum alloy 7050 is used in the upper cover, ribs, and bulkheads.

Materials

The two materials selected for extensive use in the WCTS designs are 10 Ni steel and beta annealed 6A1-4V titanium. These materials have the best combination of strength, toughness, and stress corrosion resistance that is commercially available. Their selection and properties have been discussed by Shults.[1]

10 Ni Steel

The 10 Ni steel alloy is used in the quenched and tempered condition at the 190 ksi strength level. This alloy was developed by U.S. Steel for the U.S. Navy as a candidate for HY180.[2] It is produced by the vacuum induction melting process followed by vacuum arc remelting (VIM-VAR). Fine grain practice is used to assure that all products have an ASTM grain size of 7 or finer. Tight chemistry controls are required on all residual elements. The VIM-VAR ingot is extensively cross-rolled to minimize mechanical anisotropy. The resulting steel has fracture toughness and stress corrosion resistance that are superior to any other steel alloy at the 190 ksi strength level. The material is procured to a guaranteed minimum Charpy V-notch impact toughness of 60 ft-lb.

Beta Annealed 6A1-4V Titanium

Beta annealed 6A1-4V titanium plate in the mill annealed condition was used as the primary titanium alloy. The material used was surplus from the Supersonic Transport (SST) Program. It was produced to a rigorous specification developed for the SST by the Boeing Company.[3] Beta annealing is conducted at 1850 to 1900°F for nominally 5 min. followed by cooling at a minimum rate (for plate up to 2 in. thick) of 150°F/min. In order to promote a fine-grained struture, the plates are worked in the alpha-beta temperature range prior to beta annealing. The microstructure consists of a Widmanstatten morphology with no primary alpha phase. Tighter chemistry controls are specified for oxygen (0.13 w/o max) and aluminum (5.5—5.3 w/o). Adherence to these controls coupled with good mill practice results in the most fracture resistant titanium alloy currently available. This material is supplied to a minimum guaranteed fracture toughness of 80 ksi $(in.)^{1/2}$

Stress Analysis

Finite element procedures were used extensively in the stress analysis task. This permitted efficient and accurate analyses of a number of different designs. Two different approaches were used in the analysis procedures. Overall WCTS models were constructed using single-purpose, efficient procedures with simple, constant-strain finite elements. This permitted many different models to be constructed and allowed several iterations to be run for moderate cost. A typical WCTS model is shown in Fig. 3. Models were constructed and run for local areas of greater concern using more sophisticated elements and procedures. These local models were used to study areas of rapidly varying stresses and to predict buckling loads for structural components.

Fail-safe analysis requirements impose additional challenges for stress analysis methods. The residual strength of a structure with a failed element can be easily evaluated by use of the finite element models used to analyze the basic structure. Finite elements can be altered to simulate failure conditions so that the influence on adjacent elements can be determined. Alteration of the elements may consist of simply reducing the thickness and/or the modulus of elasticity of an element to render it ineffective. It is sometimes desirable to use an orthotropic plate element which can react loads only in desired directions to simulate element or joint failures.

The dynamic effect of element failures was considered in a limited analytical investigation to predict the transient response during failure. This analysis was performed using the NASTRAN[4] procedure and consisted of the following steps: 1) a finite element analysis was performed with the structure intact; 2) the finite element model was altered to represent a failed structure and a second "residual strength" analysis was made; 3) the differences in node point loads were determined for the two models; 4) the differences in node point loads were superimposed on the nodes of the intact model as step-function loads and the transient response was determined using the direct approach option of NASTRAN.

Results of this analysis indicated peak transient stresses in various elements as much as 25 to 30% above the residual stresses. It was of interest to note that the critical element showed an increase of only 16% above the residual stress level. The analysis was conservative since the incremental loads were applied as step functions. Component tests of materials with high fracture toughness have failed to generate rapidly growing cracks which would cause a dynamic problem.

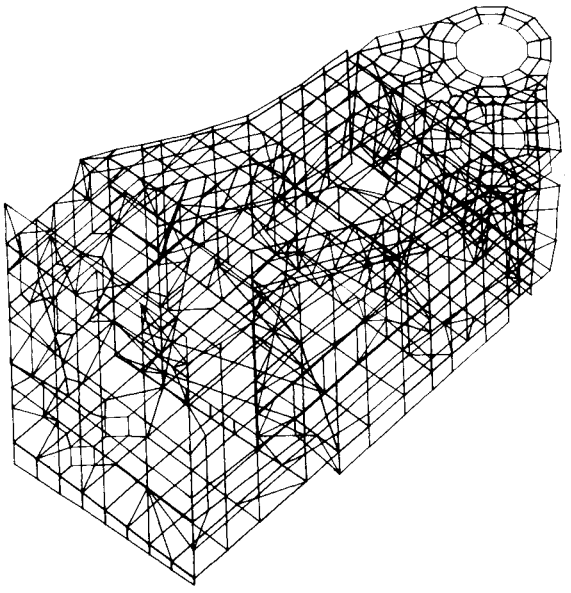

Fig. 3 Typical math model of the wing carrythrough structure.

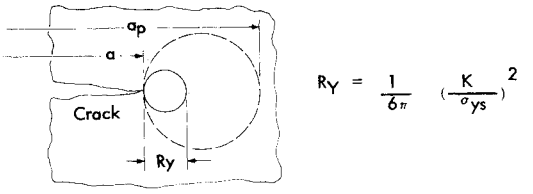

Fig. 4 Crack tip plastic zone geometry. $R_y = 1/6\pi\,(K/\sigma_{ys})^2$.

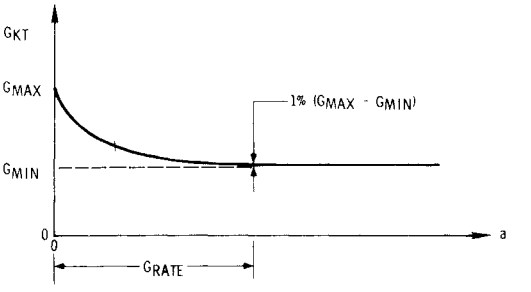

Fig. 5 Stress gradient model. $G_{kt} = G_{min} + (G_{max}\text{-}G_{min})$ exp $[ln\ (0.01)\ (a/G_{rate})]$.

An alternate approach, which was presented in the discussion of the damage tolerance requirements, was actually used to account for the dynamic effect. However, this study did demonstrate the feasibility of an analytical evaluation of the dynamic response.

Crack Growth Analysis

Crack growth analyses were conducted on both WCTS designs using the results of the stress analysis, the fatigue loads spectrum and fracture mechanics test data. The Wheeler[5] retardation model was used to account for spectrum retardation and environmental effects to the extent observed in the spectrum-environmental test program.

A modified version of the Air Force computer program CRACKS[6] was used for the crack growth analyses. The CRACKS program is based on a linear accumulation of incremental crack growth, i.e.

$$\frac{da}{dN} = f(\Delta K) \tag{1}$$

$$a_n = a_0 + \sum_{i=1}^{n} \left(\frac{da}{dN}\right)_i \tag{2}$$

where a_0 = initial crack length, a_n = crack length after n cycles.

The functional relationship between crack growth rate, da/dN, and the stress intensity range, ΔK, is established empirically from the constant amplitude crack growth test data. This relationship is expressed in terms of one or more equations of either the Paris[7] or the Forman[8] type. Environmental-enhanced crack growth is accounted for by use of the appropriate da/dN data.

The Wheeler model was used to account for spectrum retardation effects, i.e., the growth rate reduction following a peak overload. The Wheeler model was incorporated into the CRACKS program by modifying Eq. (2) as follows:

$$a_n = a_0 + \sum_{i=1}^{n} C_{Pi} \left(\frac{da}{dN}\right)_i \tag{3}$$

where C_{Pi} is the spectrum retardation factor

$$C_{Pi} = \left[\frac{R_Y}{a_p - a}\right]^m \text{ for } a + R_Y < a_p$$

$$C_{Pi} = 1 \quad \text{for } a + R_Y \geq a_p \tag{4}$$

where a, a_p and R_Y are defined in Fig. 4.

The retardation exponent, m, is an empirical constant determined on the basis of the spectrum environmental crack growth tests. The best-fit m value is obtained by generating a family of crack growth curves using the test spectrum, the appropriate da/dN data and a series of m values. The analysis curve that most closely approximates the experimental data sets the m value.

Equation (3) implies cycle-by-cycle summation of the incremental crack growth. To improve efficiency, the CRACKS program uses a Runge-Kutta integration of the da/dN curves over an interval of fatigue cycles at a constant load level within the fatigue spectrum. This procedure is extremely accurate but requires several computational steps. Further efficiency improvements were achieved for the AMAVS program by using s single-step integration procedure, i.e.

$$a_n = a_0 + \sum_{i=1}^{EN} C_{Pi} \left(\frac{da}{dN}\right)_i \Delta N_i \tag{5}$$

where ΔNi is the number of cycles in the i^{th} spectrum load level and the incremental crack growth within each load level is summed over the range of load levels applied ($i = 1$ to EN).

Use of Eq. (5) resulted in a four-fold savings in computer run time; however, computer run times were still too long. Satisfactory length computer runs (approximately 1 min/1280 flights) were achieved by converting the flight-by-flight spectrum to a 10-flight-block spectrum. Comparative runs indicated that crack growth rates were essentially the same for both spectra. The block spectrum was slightly conservative because more retardation occurred in the flight-by-flight spectrum.

An exponential decay model was used to account for the stress gradients adjacent to holes and other stress concentrations.[9] The stress intensity within the stress gradient is computed by factoring the average stress by G_{KT} as follows:

$$K = G_{KT}\sigma\ (\pi a)^{1/2} f(a)$$

where G_{KT} is the geometric stress concentration factor, $f(a)$ is the geometry correction factor. The value of G_{KT} is a function of crack length:

$$G_{KT} = G_{MIN} + (G_{MAX} - G_{MIN}) e^{Ln(0.01)\frac{a}{G_{RATE}}}$$

This equation results in an exponential decay over a characteristic length of G_{RATE} as shown schematically in Fig. 5. For

Table 1 Fatigue crack growth parameters (Forman equation) for 10 Ni steel[a]

Load ratio R	ΔK Range	Parameters $C\times10^{-8}$	Parameters n	Environmental factor, γ Dry air	Sump water @6 cpm	Sump water @60 cpm
$R<0.5$	$\Delta K<15$	4.34	3.3	1	1	1.0
$R<0.5$	$\Delta K\geq15$	294	2.0	1	2	1.5
$R\geq0.5$	All ΔK	25.2	2.2	1	2	1.5

[a]For $0.3<R<0.5$, use $R=0.3$; for $R<$, use $|R|$.

Table 2 Fatigue crack growth parameters (Paris equation) for beta annealed 6 AL-4V Titanium[a]

Load ratio R	ΔK Range	*Parameters* c	n	Environment
0.1	$\Delta K<15$	7.96×10^{-14}	6.4	Dry air
0.1	$\Delta K\leq15$	2.08×10^{-10}	3.5	Dry air
0.3	$\Delta K<15$	6.60×10^{-12}	4.9	Dry air
0.3	$15\leq\Delta K\leq42$	6.39×10^{-10}	3.2	Dry air
0.3	$\Delta K<42$	2.08×10^{-10}	3.5	Dry air
0.5	$\Delta K<12.5$	1.60×10^{-10}	3.9	Dry air
0.5	$\Delta K\leq12.5$	1.30×10^{-9}	3.07	Dry air
0.1	$\Delta K<20.9$	7.96×10^{-14}	6.4	Sump tank water
0.1 and 0.3	$20.9\leq\Delta K\leq42$	3.24×10^{-8}	2.15	Sump tank water
0.1 and 0.3	$\Delta K<42$	2.08×10^{-10}	3.5	Sump tank water
0.3	$\Delta K\leq20.9$	6.54×10^{-12}	4.95	Sump tank water
0.5	All ΔK	1.60×10^{-10}	3.9	Sump tank water

[a]For $R<0.5$ use $R=0.5$ data; for $0.1<R<0.3$ and $0.3<R<0.5$, interpolate; for $0\leq R\leq0.1$, extrapolate; for $R<0$, use $|R|$.

cracks adjacent to holes; $G_{MAX}=3.0$, $G_{MIN}=1.0$, and G_{RATE} = the hole diameter. For other stress concentrations; G_{MAX}, G_{MIN}, and G_{RATE} are selected to closely simulate the gradient.

Fatigue Crack Growth Test Data

The fatigue crack growth behavior of beta annealed 6A1-4V titanium and 10 Ni steel was evaluated under constant amplitude and flight-by-flight spectrum loading conditions. Constant amplitude tests using compact tension *(CT)* and wedge-opening-load *(WOL)* specimens were conducted in dry air at 360 cpm and in sump tank water at 6 and 60 cpm.

The constant amplitude test results for 10 Ni steel have been expressed as Forman equations having the following form:

$$\frac{da}{dN}=\frac{C(\Delta K)^n\gamma}{(1-R)200-\Delta K}$$

where da/dN = crack growth rate, K = stress intensity range, γ = environmental factor, R = load ratio; min load/max load, c,n = empiricial parameters. The range of applicability of the empirical parameters used to fit the test data is summarized in Table 1. The analytical curves are shown with the test results in Figs. 6 and 7. For the $R=0.1$ tests in sump water, there is a significant reduction (relative to corresponding tests in dry air) in growth rates at ΔK levels below 20 ksi (in.)$^{1/2}$. The reduced growth rates are attributed to rust deposits on the fracture surface which limited the crack opening displacement range.

The constant amplitude test results for beta annealed 6A1-4V titanium have been expressed as Paris equations having the following form: $da/dN=C(\Delta K)^n$. The ranges of applicability of the empirical parameters used to fit the test data are summarized in Table 2. The analytical curves are shown with the test results in Figs. 8 and 9. Crack growth rates for intermediate R ratios were determined by interpolation or extrapolation for use in spectrum crack growth analysis. The crack growth data obtained in a sump tank water environment

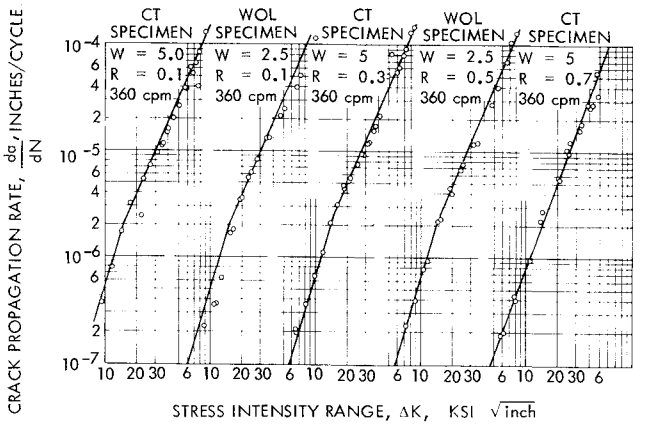

Fig. 6 Fatigue crack growth behavior of 10 Ni steel in dry air.

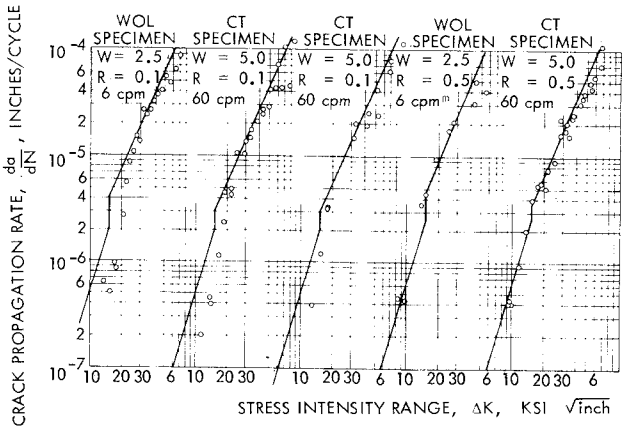

Fig. 7 Fatigue crack growth behavior of 10 Ni steel in pump tank water.

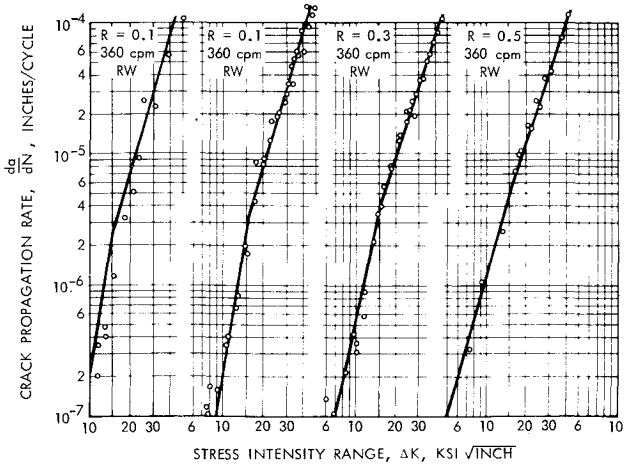

Fig. 8 Fatigue crack growth behavior of beta annealed 6A1-4V titanium in dry air. CT specimen $W=5$.

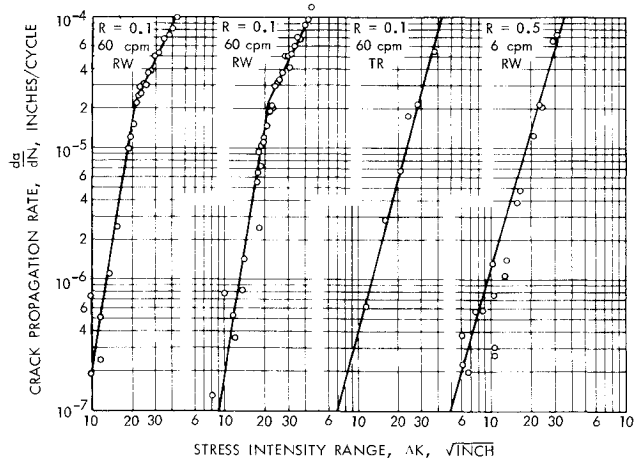

Fig. 9 Fatigue crack growth behavior of beta annealed 6A1-4V titanium in sump tank water. CT speciment, $W=5$.

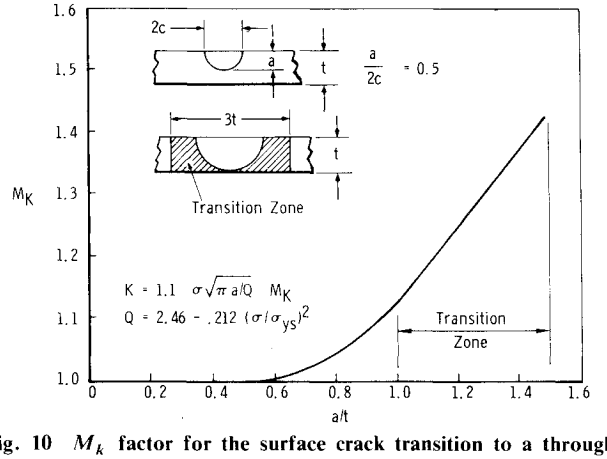

Fig. 10 M_k factor for the surface crack transition to a through-thickness crack.

were not simply related to the corresponding dry air data as was the case for 10 Ni steel. Consequently, it was necessary to have separate data libraries for the two different environments instead of using the environmental factor approach.

Flight-by-flight spectrum-load fatigue tests were conducted using tensile panels with either surface flaws or cracked holes. Specimens were tested under four distinct spectra representing two structural locations and two truncation levels as summarized in Table 3. The test results were analyzed using the

Table 3 Spectrum crack growth test program

Environment	Spectrum	Specimen
Dry air	1	SF
Dry air	2	SF
Dry air	1	CH
Dry air	2	CH
Dry air	1*	SF
Dry air	2*	SF
Sump	1	SF
Tank	1*	SF
Water	2*	SF

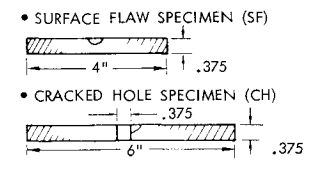

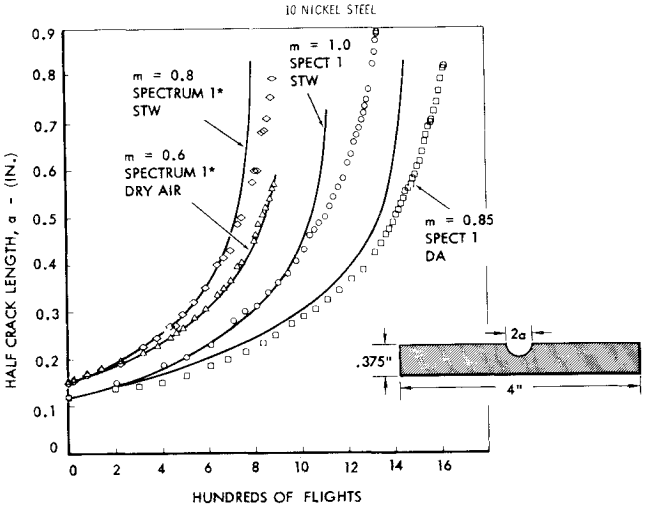

Fig. 11 Spectrum crack growth behavior of 10 Ni steel, spectra 1 and 1*.

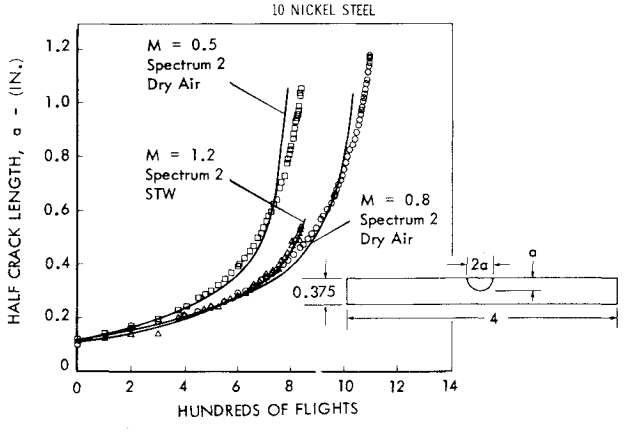

Fig. 12 Spectrum fatigue crack growth behavior of 10 Ni steel, spectra 2 and 2*.

constant amplitude crack growth data, the appropriate stress intensity functions and the Wheeler crack growth analysis model. The stress intensity, K, functions were as follows:

$K = 1.1\sigma(\pi a/Q)^{1/2}M_K$ for surface cracks

where $Q = \Phi^2 - 0.212\,(\sigma/\sigma_{ys})^2$

M_K = back face correction factor,

σ = applied stress

σ_{ys} = 0.2% offset yield strength

a = crack length

Φ = shape factor = 1.57 for semicircular cracks

$K = 1.2\sigma(\pi a/Q)^{1/2}M_K G_{KT}$ for cracked holes were G_{KT} = stress gradient factor, and

$K = \sigma(\pi a/m)^{1/2}(\sec \pi a/w)^{1/2}\,\sigma(\pi a/m)^{1/2}$ for through cracks where w = panel width.

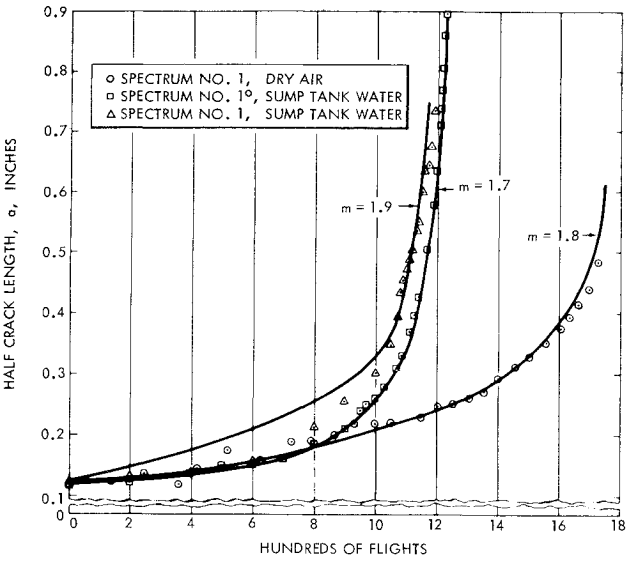

Fig. 13 Spectrum fatigue growth behavior of beta annealed 6A1-4V titanium, spectra 1 and 1*.

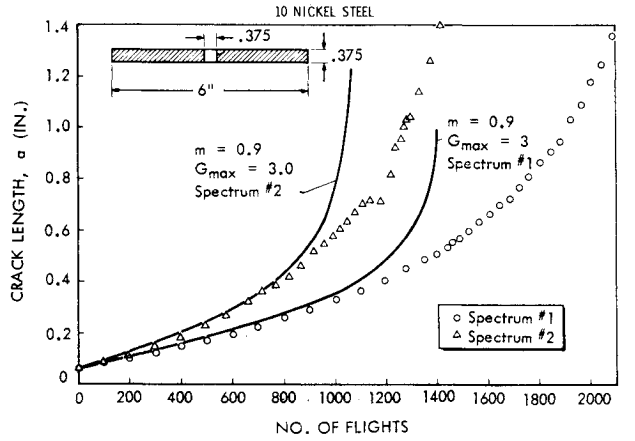

Fig. 14 Spectrum fatigue crack growth behavior of cracks adjacent to holes in 10 Ni steel.

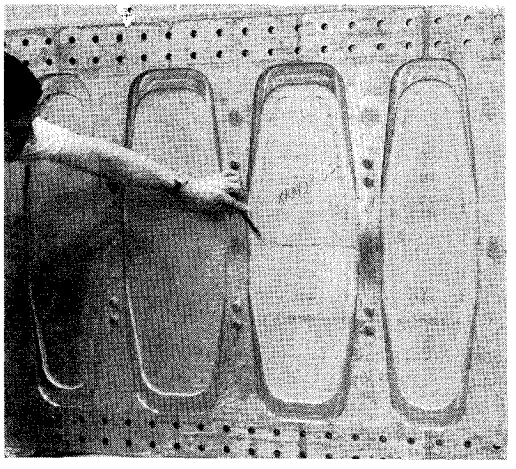

Fig. 15 Brazed fail-safe titanium specimen after application of 3,000,000 lb ultimate load.

The transition from a part-through crack to a through-thickness crack was assumed to occur over a range of crack lengths varying from $2c=2t$ $(a/2c=0.5)$ to $2c=3t$. This assumption was treated analytically by use of the surface crack equation until $2c=3t$, with M_K varying as a function of a/t as shown in Fig. 10. The value of M_K at $2c=3t$ was selected such that continuous K values were obtained at transition.

Table 4 Spectrum fatigue crack growth test results for beta annealed 6 AL-4V titanium

Environment	Spectrum	Specimen	m
Dry air	1	Surface flaw	1.8
Dry air	2	Surface flaw	1.6
Dry air	1	Cracked hole	1.4
Dry air	2	Cracked hole	0.7
Sump tank water	1	Surface flaw	1.9
Sump tank water	1*	Surface flaw	1.7
Sump tank water	2*	Surface flaw	1.8

The spectrum load fatigue test results for 10 Ni steel surface flaw test specimens are presented in Figs. 11 and 12. Values for the retardation exponent, m, ranged from 0.5 to 1.2. In the dry air tests, the Wheeler model adequately accounted for the differences in spectra 1 and 2 and in spectra 1* and 2*, i.e., the m value was nearly constant. However, significant changes in m were required to account for spectrum truncation and environmental effects.

The spectrum load fatigue test results for beta annealed 6A1-4V titanium are summarized in Table 4. For surface flaw specimens, the m-value ranged from 1.6 to 1.9. This is considered very close correlation between test and analysis and adequate accounting for spectrum truncation and environmental effects. The crack growth curves for spectrum 1 in dry air and sump tank water and for spectrum 1* in sump tank water are shown in Fig. 13.

For cracks adjacent to holes, the correlation between test and analysis was nil at crack lengths greater than 0.375 in. The correlation obtained for 10 Ni steel is shown in Fig. 14. A similar lack of correlation was obtained for beta annealed 6A1-4V titanium. This cannot be attributed to the stress gradient model because the model is only applicable for 1 hole diameter, 0.375 in. in this case. The lack of correlation was apparently due to overestimation of the stress intensity as the crack transitioned from a 0.375 in. surface flaw to a through-thickness crack adjacent to a hole. Load transfer to the uncracked side of the hole (the stiffer load path) was not accounted for in the analysis and may have been the principal source of error.

Evaluation of the WCTS Designs

The damage tolerance of the WCTS designs was evaluated by component tests, fail safe analyses, and safe crack growth analyses. In general, the most cirtical locations of each design were identified, evaluated, and found to meet the damage tolerance requirements. By implication, the less critical areas exceeded the requirements.

A variety of component tests discussed by Hart and Boensch[10] were conducted to evaluate the static strength, fatigue life, and damage tolerance of the designs. The fail safe tests on the brazed lower plate were the only tests that specifically evaluated damage tolerance. This test series, described in detail in Ref. 11, was culminated with a full scale specimen simulating the outboard portion of the lower plate. An 11.75 in. initial crack was successfully contained for ¼ service life of fatigue cycling followed by application of ultimate load (3,000,000 lbs.). The specimen, after completion of testing, is shown in Fig. 15.

Residual strength analyses were performed on the brazed lower plate of the fail safe titanium design for a number of different failed elements. The largest failure considered was a 30 in. crack in the center element of the lower plate (two bays). The bar elements between the two bays were left intact and developed the highest residual stress, which approached F_{tu} of the material at limit load. Results of this analysis are shown in Fig. 16.

Crack growth analyses were conducted for several critical locations of both designs using the procedures outlined

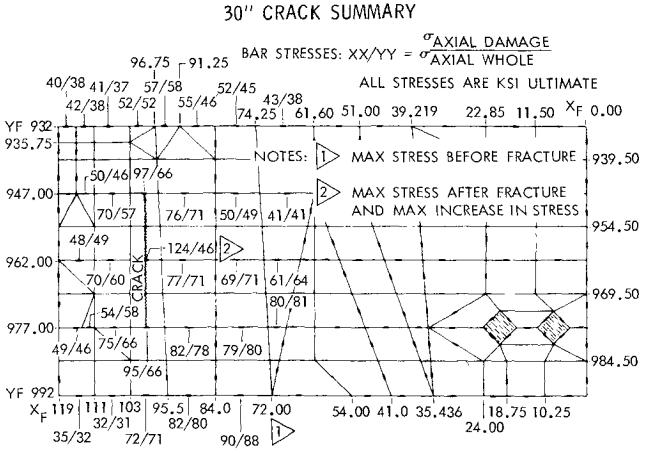

Fig. 16 Residual strength analysis of the titanium fail-safe design.

previously. For both 10 Ni steel and beta annealed 6A1-4V titanium, surface flaws in open structures were shown to readily meet the safe crack growth requirements. Cracks adjacent to holes grew much faster, but also met the safe crack growth requirements providing the stress levels were kept below the allowable stress based on fatigue analysis—100 ksi at ultimate load for beta annealed 6A1-4V titanium and 150 ksi for 10 Ni steel. Consequently, no additional weight was required to meet the safe crack growth requirements.

There were several reasons why the fatigue requirements were more critical than the safe crack growth requirements. The main reason is that a scatter factor of 4 is required on the fatigue analysis whereas a scatter factor of 1 is used in crack growth analysis. In addition, the stresses used in fatigue analysis are more severe; von Mises combined stresses on the net section are used in fatigue analysis whereas principal stresses on the gross section are used in crack growth analysis. Another important factor for this particular design is that the 10 Ni steel and beta annealed 6A1-4V titanium have relatively good crack growth resistance, but relatively poor crack initiation resistance.

Summary and Conclusions

Two WCTS configurations, a fail safe titanium design and a monolithic steel design, have been evaluated in accordance with a stringent set of damage tolerance requirements. Fracture mechanics analyses, based on extensive fatigue crack growth data, indicated that both designs meet the safe crack growth requirements. In addition, material and component tests indicate that both designs have a very high degree of inherent damage tolerance due to the excellent fracture resistance of beta annealed 6A1-4V titanium and 10 Ni steel.

References

[1] Shults, J. M., "Material Selection and Evaulation for Advanced Metallic Aircraft Structures," AIAA Paper 74-373, Las Vegas, Nev., 1974.

[2] Porter, L. F., "Final Report—Preliminary Development of a HY180 Weldment System," Rept. 39.018-007(52), Aug. 16, 1971, U.S. Steel Applied Research Laboratory.

[3] Jensen, G. A. and Eichenberger, T. W., "SST Technology Follow-on-Program—Phase I, Titanium Alloy 6A1-4V Mechanical Property Data," Rept. FAA-SS-72-02, March 1972,.

[4] McCormick, C. W., "The NASTRAN User's Manual," SP-222, 1970, NASA.

[5] Wheeler, O. E., "Spectrum Loading and Crack Growth," *Transactions of the ASME Journal of Basic Engineering,* March 1972.

[6] Engle, R. M., "CRACKS, A Fortran IV Digital Computer Procedure for Crack Propgation Analysis," AFFDL-TR-70-107, Oct., 1970, Wright-Patterson Air Force Base, Ohio.

[7] Paris, p. C., "The Fracture Mechanics Approach to Fatigue,"- *Proceedings of the Tenth Sagamore Army Materials Research Conference,* Syracuse University Press, Syracuse N.Y., 1964.

[8] Forman, R. G., Kearney, V. E., and Engle, R. M., "Numerical Analysis of Crack Propagation in Cyclically Loaded Structures,"- *Transactions of the ASME, Journal of Basic Engineering,* Vol. 89, No. 3, 1967, p. 459.

[9] Wheeler, O. E., unpublished Research, 1969.

[10] Hart, C. E. and Boensch, F. D., "The Advanced Metallic Air Vehicle Structure Program," AIAA Paper 74-337, Las Vegas, Nev., 1974.

[11] McHenry, H. I. and Key, R. E., "Brazed Titanium Fail Safe Structures," *Welding Journal,* sumbitted for publication.